Wear 267 (2009) 619–624

Contents lists available at ScienceDirect

Wear

journal homepage: www.elsevier.com/locate/wear

Multifunctionality of single-walled carbon nanotube–polytetrafluoroethylene nanocomposites

J.R. Vail [a], D.L. Burris [b,*], W.G. Sawyer [a]

[a] University of Florida, Gainesville, FL, USA
[b] University of Delaware, Newark, DE, USA

ARTICLE INFO

Article history:
Received 30 July 2008
Received in revised form
23 December 2008
Accepted 24 December 2008

Keywords:
Nanocomposite
Dispersion
Interface
Polytetrafluoroethylene (PTFE)
Space
Solid lubrication

ABSTRACT

Multifunctional nanocomposites are increasingly needed for applications requiring prescribed sets of physical and chemical properties. Polytetrafluoroethylene (PTFE) is a popular solid lubricant due to its low friction coefficient, high chemical inertness, high thermal range and biocompatibility, but its use is limited by high rates of wear. Low loadings of nanoparticle fillers have reduced PTFE wear by 3–4 orders of magnitude, but these materials lack the mechanical, electrical or thermal properties needed for high performance applications. In this study, single-walled carbon nanotubes (SWCNT) are investigated as a route to improve wear resistance, toughness and electrical conductivity of PTFE without sacrificing low friction, high temperature capability or chemical inertness. Tribological, tensile and surface electrical measurements were made for 0, 2, 5, 10 and 15 wt.% SWCNT filled PTFE nanocomposites. A dramatic reduction in electrical resistance reflected networking (percolation) of the nanotubes at 2 wt.%. All of the nanocomposites had significantly improved electrical, mechanical and wear performance. Above 2 wt.%, electrical conductivity was reduced by more than six orders of magnitude. At 2 wt.%, ultimate engineering stress was improved by approximately 50%, true stress increased by 200%, engineering strain increased by two orders of magnitude (~10,000%). At 5 wt.%, wear resistance improved by more than 20 times and friction coefficient increased by ~50%.

1. Introduction

Polymeric composites offer design engineers a wide range of tunable physical properties and are frequently used in high performance applications. Polymer matrix composites filled with various forms of carbonaceous material (*e.g.* carbon fiber) are common and generally possess very high strength, stiffness, and thermal conductivity per unit weight. As a group they are suitable for high performance applications where a prescribed set of properties (multifunctionality) is needed. Frequently, they are used as structural materials, but do occasionally have applications in tribology.

Carbon nanotubes (CNTs) are of increasing interest in this area. These nanomaterials have diameters on the 1–10s nm size scale, lengths on the order of microns and an unrivalled combination of mechanical, thermal, chemical and electrical properties. As a result, these fillers have enormous potential for use in nanostructured materials with tunable multifunctionalities. A large number studies have already been conducted on these unique materials, and while impressive practical improvements in wear, friction, electrical conductivity, strength and toughness have been observed [1–3], theoretical studies suggest that the full potential of carbon nanotubes has yet to be extracted [4–6].

Tribology is a particular area in need of novel multifunctional materials. Tribological components must reliably provide low friction with minimal wear and deformation, conduct frictional heat, carry large normal stresses, and in some cases, conduct electrons. Moving mechanical assemblies in space, for example, rely upon a variety of gears, bearings, gimbals, latches, motors and slip-rings for remote operation in hard vacuum and thermal extremes that preclude traditional lubrication strategies. The unique challenges of space operation have motivated significant research efforts aimed at the development of multifunctional solid lubricants for extended use in a broad range of extreme environments [7–18].

Polytetrafluoroethylene, with low friction, low outgassing, high chemical inertness and high temperature capability, is an ideal candidate for space applications, but high wear rates preclude its use in many cases. Low loadings of alumina nanoparticles have produced remarkable reductions in the wear of PTFE [8,19,20], but these particles lack the favorable thermal, mechanical, and most importantly, geometric attributes of CNTs. Chen et al. [21] previously examined the wear characteristics of CNT–PTFE nanocomposites, but wear improvements were relatively modest. The role of nanotube dispersion, chemistry and structure in preventing large-scale damage of

* Corresponding author at: University of Delaware, Mechanical Engineering, 126 Spencer Lab, Newark, DE 19716, USA. Tel.: +1 302 831 2006.
E-mail address: dlburris@udel.edu (D.L. Burris).

0043-1648/$ – see front matter © 2009 Elsevier B.V. All rights reserved.
doi:10.1016/j.wear.2008.12.117

PTFE remain unclear. In this paper, SWCNT–PTFE nanocomposites were created and tested to further explore the potential synergies between the unique property sets of the constituents and the mechanisms responsible.

2. Experimental methods

The matrix material used in this study was Polytetrafluoroethylene (PTFE, Teflon™ 7C from DuPont) compression molding resin with an average particle size of approximately 30 μm. The filler materials were single-walled carbon nanotubes, SWCNTs (Elicarb™ from Thomas Swan & Co.); these nanotubes have average reported diameter and length of 2 nm and 5 μm, respectively. Fig. 1 (left) shows a transmission electron microscopic (TEM) image of the as-received nanotubes following 1 h of ultrasonication in isopropyl alcohol. Surveying revealed diameters between 2 and 20 nm. Despite efforts to disband agglomerations using ultrasonication, the nanotubes were found to be tangled with individual tubes only being distinguishable at the edges of agglomerates. Effective nanotubes dispersion is clearly a major technological barrier in this area and the impact of dispersion on nanocomposite properties remains poorly understood.

Prior to processing, the SWCNTs were classified using a 40 mesh sieve; only powders that easily passed were processed further. The sieve classified nanotubes, glass beads (grinding media) and ethanol (suspension and cooling medium) were combined and mixed mechanically in a Hauschild Speed Mixer as described in McElwain et al. [19,20] at high speed (3000 RPM) for 10 min. Following mechanical mixing, the container was ultrasonically mixed for 30 min; the beads were then removed and the ethanol evaporated. Appropriate masses of the SWCNTs and PTFE Teflon™ 7C were combined to achieve 0, 2, 5, 10 and 15 wt.% SWCNT–PTFE mixtures. The powder ensembles were combined with ethanol, mechanically mixed at high speed for 5 min, then ultrasonically dispersed for 10 min and allowed to dry overnight at 60 °C in rough vacuum. An image of the dispersed and dried powder ensemble at 5 wt.% loading is shown in Fig. 1 (right). Following dispersion and drying, the dried powders were compression molded at 363 °C and machined into test specimens. A single 5 wt.% sample was dry dispersed to remove any potential effects of the ethanol. Appropriate weights of sieved powders were combined and dispersed using the high energy jet-mill described in Sawyer et al. [22]. The jet-mill uses high velocity air to impact the powders and break agglomerations. A single 5 wt.% C_{60} sample was created using the mechanical mixing/ultrasonication procedure to isolate the geometric effects of the nanotubes.

Relative reductions in surface resistance of samples that were 13 mm in diameter by 6.5 mm in thickness were measured using a Keithley 2400 SourceMeter. Two electrodes of 100 μm contact radius were randomly placed on the sample with a separation of no less than 6 mm and a potential difference of 200 V. The resistance to current flow was measured at least 40 times per sample in random locations.

Bulk mechanical properties of unfilled PTFE and 2 wt.% SWCNT were tested using an MTS 858 Mini Bionix II. A dog-bone shaped specimen was necessary for static gripping of the low friction samples; the final CNC samples had a thickness of 2.5 mm. One-eighth inch radii provided a transition from the 15.5 mm long by 4.4 mm wide test area to the 8 mm long by 10 mm wide grip area without introducing significant stress concentration. Tests were performed in open laboratory air at an extension rate of 1 mm/min.

The linear reciprocating tribometer described in Schmitz et al. [23,24] was used to quantify wear and friction. The apparatus is contained in a soft-walled clean room and exposed to air of ~25% relative humidity. Each test used a new rectangular flat counterface of lapped (150 nm R_a) 304 stainless steel which was mounted to the linear reciprocating stage. The 6.3 mm × 6.3 mm × 12.7 mm tribology samples were mounted directly to a 6-channel load cell. A normal force of 250 N was applied using a pneumatic cylinder/linear thruster assembly. The sliding velocity was nearly constant at ±50.8 mm/s over the 25.4 mm reciprocation length.

Mass loss measurements were made to eliminate the confounding effects of elastic deformation, creep and thermal distortions on dimensional wear measurements. Analytical expressions for single point wear measurements are obtained using the individual measurement uncertainties and e *law of propagation of uncertainty* as described by Schmitz et al. [23]. However, solid lubricants often exhibit a reduction in wear rate as transfer films set up; least squares regressions of the steady data are needed to obtain steady-state wear rates. This wear measurement method complicates the calculation of wear rate uncertainty. At each measurement, the nominal measured value (average) and the uncertainty in that measurement (standard deviation) are calculated for volume loss and the product of normal load and sliding distance. One thousand data sets are simulated using the measurement as the average and uncertainty as the standard deviation (Monte Carlo simulation). Regression slopes are calculated for each of the simulated data sets; the average of these slopes is the wear rate and the standard deviation is the uncertainty.

Small filler size enables a unique potential to impact the crystalline nature of the polymer matrix. Numerous authors have reported changes in matrix properties like glass transition and degradation temperatures following nanoparticle incorporation [25–28]. Particle/polymer interfaces and their cumulative effects on the nanocomposite properties are widely discussed as potential mechanisms for property enhancement in the nanocomposites literature [1,6,29]. A previous study has shown that alumina nanofillers are effective nucleation sites for PTFE crystallization [30]. A TA Instruments Q20 differential scanning calorimeter (DSC) was used here to study potential effects of the carbon fillers on PTFE crystal nucleation. The samples were heated at 10 °C/min to 400 °C, equilibrated for 10 min and cooled at a rate of 10 °C/min. Heats of fusion were calculated from crystallization measurements during cooling.

3. Results

The averages and standard deviations of surface resistance (R) measurements of the composites are shown in Fig. 2 as a function of filler wt.%. PTFE is an outstanding electrical insulator and the true resistance is likely many orders of magnitude greater than the detection limit of the instrument. At 2 wt.%, detectable electrical currents were observed in 16 of 45 measurements indicating that the nanotubes were networked over large regions within the nanocomposite (percolation). As illustrated in Fig. 1 (right), the high aspect ratio (length:width) of the nanotubes provides a high probability for contact between nanotubes at low loadings. From 5 to 15 wt.% SWCNT, the resistance continued to decrease but was far less sensitive to probe locations and SWCNT loading. At 5 wt.%, jet-milled and ultrasonicated samples had identical mean resistance. The scatter in the measurements, however, was much smaller for the jet-milled sample suggesting improved homogeneity in the networking from improved nanotube dispersion.

These results are qualitatively and quantitatively consistent with previous studies of nanotube percolation in the polymer nanocomposites literature [3,31,32] and indicate reasonable dispersion despite the added challenges introduced by the PTFE matrix (PTFE cannot be melt-mixed nor can particles be dispersed in a liquid monomer prior to polymerization). Spherical C_{60} fillers, with an identical sp^2-bonded graphene structure, lack the bene-

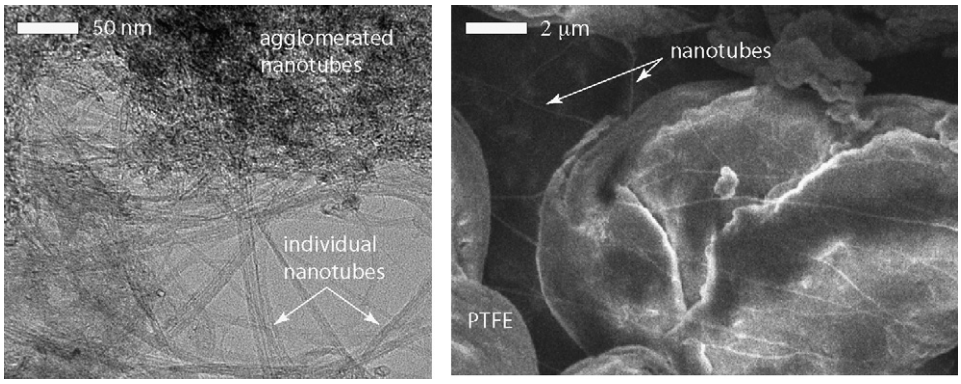

Fig. 1. Materials used in the study. (Left) Elicarb single-walled carbon nanotubes (SWCNTs). A typical nanotube agglomerate is located at the top of the image and individual nanotubes are found at the edge toward the bottom. (Right) Ultrasonic dispersion of 5 wt.% SWCNT–PTFE. The nanotubes can be seen decorating the ~15–30 μm PTFE particles.

ficially high aspect ratios of CNTs, and as a result, the probability for inter-particle networking (percolation) is only appreciable at high loadings. Ltaief et al. [33] demonstrated that C_{60} percolation occurred at approximately 40 vol.% filler loading. No measureable currents were detected for the 5 wt.% C_{60}–PTFE nanocomposite in this study, which demonstrates that low loading networking is purely due to the structural benefits of the nanotubes.

The results of uniaxial tensile experiments in Fig. 3 show that 2 wt.% SWCNTs had a dramatic effect on the mechanical properties of PTFE. The unfilled PTFE had a maximum engineering stress of σ = 7.67 MPa and an engineering strain at failure of ε = 4.81%. With 2 wt.% SWCNTs, the maximum engineering stress was increased by more than 50% and the engineering strain to failure increased by nearly two orders of magnitude. Portions of the sample lost load carrying capacity around 120% strain; interestingly, the material recovered after continued extension and load carrying capacity increased until the strain reached ~220% strain.

Friction coefficients and volume losses are plotted versus sliding distance in Fig. 4. At these conditions, the friction coefficient of unfilled PTFE was initially equal to 0.13 and decreased monotonically throughout the test. The friction coefficient approached 0.11 as the sample became too worn for further testing. The addition of 2 wt.% or more SWCNT increased the friction coefficient significantly. The friction coefficient of each sample varied with loading and sliding distance as wear debris and transfer films were generated.

Unfilled PTFE wore down at an excessive rate, losing 29.5 mm^3 within the first 250 m of sliding. The addition of 2–15 wt.% SWCNT increased wear resistance significantly, with each of the nanocomposites requiring well over an order of magnitude longer distances for comparable wear losses. The 2 and 5 wt.% samples had brief periods of higher transient wear rates followed by lower steady-state wear rates, while the 10 and 15 wt.% samples did not have measureable wear transients.

Friction coefficient and wear rate are plotted versus filler wt.% in Fig. 5. The data from Chen et al. [21] have been reproduced for comparison. With greater sliding speed, Chen et al. reported significantly higher friction coefficients for unfilled PTFE. This reflects the well-documented speed dependence of the unfilled polymer [34–37]; as Makinson and Tabor describe [35], the amorphous polymer separating crystalline striae are more easily sheared at lower rates. At higher rates, these regions become less mobile, and other higher friction slip pathways are activated. Despite the large speed difference between studies, the CNT–PTFE nanocomposites had comparable values of friction coefficient. Following the completion of the wear test, the 5 wt.% sample was tested from 13 to 130 mm/s to directly probe the speed sensitivity. The friction coefficient varied by less than 10%, thus confirming substantially reduced speed sensitivity.

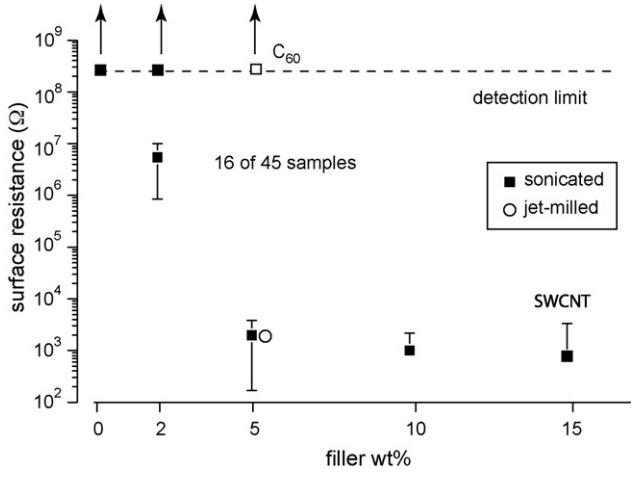

Fig. 2. Surface resistance plotted versus filler loading for PTFE composites. The black squares represent sonicated SWCNT samples. Jet-milling had no effect on the average resistance, but the dispersion in resistance measurements was substantially lower and is suggestive of the dispersion differences. Not surprisingly, C_{60} did not enable electron conduction to a measureable extent. Confidence intervals represent the standard deviation of averaged data collected during the test.

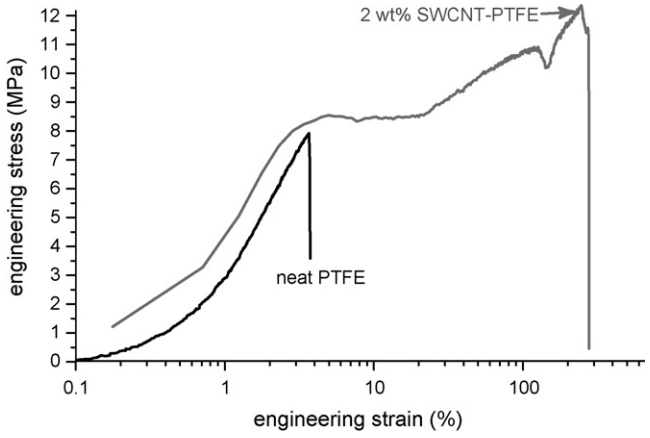

Fig. 3. Engineering stress plotted versus engineering strain for neat PTFE and 2 wt.% SWCNT–PTFE. Although substantial improvements in stress and strain were found with the high aspect ratio nanotubes, the benefits from alumina nanoparticles were even larger suggesting that the high aspect ratio and excellent mechanical properties of the nanotubes may be dominated by the effects of the nanoscale interfaces on the polymer itself.

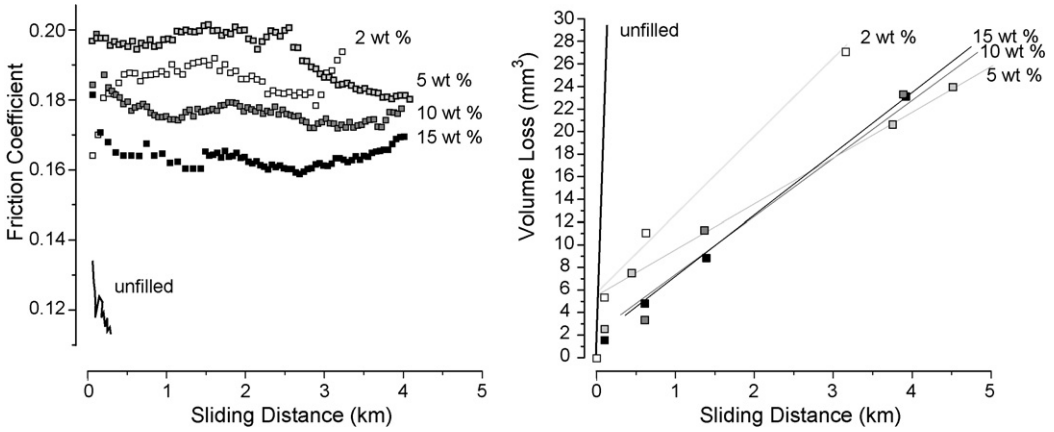

Fig. 4. Effect of sliding distance on tribological properties. (Left) Friction coefficient plotted versus sliding distance. (Right) Volume loss plotted versus sliding distance; confidence intervals representing experimental uncertainty are smaller than the data markers. Normal load was 250 N and sliding speed was 50.8 mm/s.

Wear rate is plotted SWCNT wt.% in Fig. 5 (right). With as little as 2 wt.% SWCNTs, the nanocomposites were well over 10 times more wear resistant than the unfilled polymer. Chen et al. [21] found a similar break in wear rate and hypothesized that wear improvements were the result of SWCNT entanglement with the polymer and super-strong mechanical properties of the nanocomposites. Improved mechanical properties were confirmed in this study, and although wear resistance correlates with electrical conductivity, the nanotube–PTFE interactions likely dominate nanotube–nanotube interactions. Above 2 wt.%, the nanocomposites from Chen et al. were more wear resistant. The source of the discrepancy remains unclear, but is likely related to the dispersion, nanotube quality, speed, geometry or the influence of path reversals.

DSC measurements were made to determine the effect of the nanotubes on polymer crystallinity; the results are plotted in Fig. 6. The heats of fusion from crystallization of five repeat samples of unfilled PTFE show strong repeatability at 25.5 J/g, or 21% crystallinity (based on 82 J/g for perfectly crystalline PTFE [38]). The heats of fusion of the nanocomposites decreased monotonically with increased filler loading. Since the weight of the alumina does not contribute to the signal, lines of constant crystallinity also decrease with increased loading. Despite previous findings of crystal nucleation with alumina, these DSC results suggest that the nanotubes had little or no effect on the crystallization behavior of the polymer.

4. Discussion

Based on the observation of monotonically decreased friction with SWCNT loading, Chen et al. [21] concluded that the nanotubes were self-lubricating. The results of the current study refute this hypothesis. Further, given that the crystallinity was unchanged, the observed increase cannot be attributed to a reduced presence of the low shear amorphous regions. A consistent hypothesis is that the nanotubes effectively immobilize these amorphous regions, arresting crack propagation and disabling the low friction mechanism of PTFE at lower speed. The high speed from Chen's study masked this effect. The observed decrease in friction with increase loading did not appear to be due to inherent lubricity of the filler. Rather, with increased filler loading, we observed reductions in debris size, increases in the number of debris particle, reductions in transfer film thickness and improvements in their uniformity. At 15 wt.%, the increased number of particles outweighed the reduction in size, and the wear rate actually increased. The lubricating third bodies, in this case, are believed to be SWCNT–PTFE nanocomposite transfer films and debris rather than individual nanotubes.

Despite evidence of improved dispersion under ethanol/acetone-free processing conditions, jet-milling had no significant effect on friction or wear. In fact, all of the wear reductions found here are very comparable to those published by Chen et al. in 2003 [21]. The benefits of the nanotube structure were also clearly illustrated by the wear results of the C_{60} filler; at 5 wt.%, the C_{60}

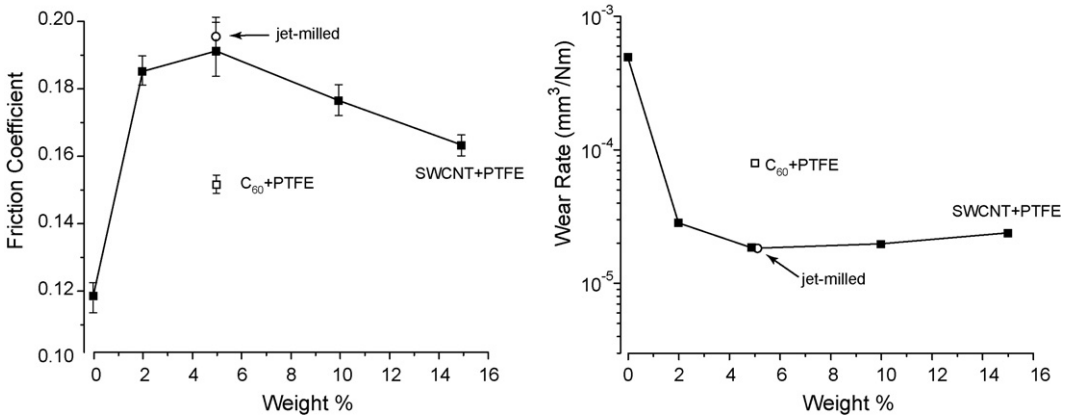

Fig. 5. Effect of filler loading on friction coefficient (left) and wear rate (right) of SWCNT–PTFE nanocomposites. Confidence intervals on friction coefficient data represent the standard deviation during the test. Confidence intervals on wear rate data represent the experimental uncertainties in both worn volume and sliding distance and are smaller than data markers in all cases. Normal load was 250 N and sliding speed was 50.8 mm/s.

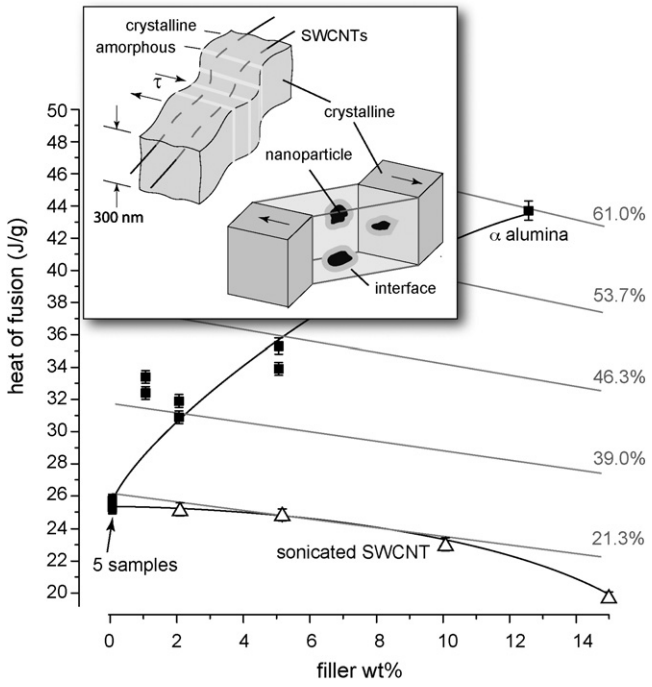

Fig. 6. Heat of fusion plotted versus filler loading. Heat of fusion is calculated from differential scanning calorimetry (DSC) of PTFE nanocomposites during recrystallization at a cooling rate of 10 °C/min. Confidence intervals represent the experimental uncertainty in the calculation of heat of fusion as described in Burris [dfdg]. Since the filler mass is involved in the calculation of heat of fusion without providing any signal input, lines of constant PTFE crystallinity are also functions of filler loading. Five samples of PTFE were processed and tested for repeatability. Above is an illustration of the semi-crystalline banded structure of the PTFE with the hypothesized immobilization mechanisms of SWCNTs and effective nanoparticles.

nanocomposite had 5× the wear rate of 5 wt.% SWCNT–PTFE sample. Chen et al. suggested that the wear improvements were the result of SWCNT entanglement with the polymer and super-strong mechanical properties of the nanocomposites. This hypothesis was reinforced here through confirmation of improved mechanical properties. Considering both the DSC and mechanical results, the mechanism of reinforcement does appear to be purely mechanical, where the most likely immobilization mechanism is the physical tethering of individual crystallites as described by Chen et al. and as depicted in Fig. 6. This hypothesis also accounts for the increased friction coefficients.

Although dramatic wear reductions were achieved due to the geometric attributes of the filler, these gains are rather modest compared to prior findings with alumina–PTFE nanocomposites. These nanocomposites were 100 times more wear resistant than comparable SWCNT–PTFE despite lacking any appreciable mechanism of mechanical reinforcement. As shown in Fig. 6, the α (hexagonal-oxygen ions, 2/3 octahedral-aluminum ions) phase alumina nanofiller in question also nucleates crystallization to a dramatic extent. Highly crystalline PTFE is not itself wear resistant [39]; increased crystallinity is simply an indication of the interaction between the particles and the polymer. The operative nanoscale wear reduction mechanism is far more efficient than purely mechanical mechanisms of wear reduction [40–42].

The importance of surface chemistry and interfacial compatibility are widely recognized in the polymer nanocomposites literature [6]. As a result, there has been increased focus on the design of the interface via nanoparticle coatings. Nanoparticle and nanotube coatings have been shown to enhance the interfacial compatibility and improve properties like load support and thermal stability [1,26,29,43,44]. The incorporation of SWCNTs into a PTFE matrix demonstrated novel multifunctionality though dramatic improvements in conductivity, toughness and wear resistance, but wear improvements were limited because the nanotubes lack the surface characteristics needed for strong interaction with the polymer. Alumina nanofillers are remarkably efficient PTFE wear reducers, but they lack the geometric properties needed for other functionalities like thermal and electrical conductivity. These studies suggest that an ideal PTFE filler is α phase alumina coated nanotubes. Low loadings of these fillers are expected to have an enormous impact on wear resistance, strength and thermal conductivity while retaining the attractive functionalities of the PTFE.

5. Conclusions

This paper reports on the electrical, mechanical and tribological properties of SWCNT–PTFE nanocomposites. The nanocomposites demonstrated multifunctionality that is only possible with the unique chemical, mechanical, electrical and structural properties of the nanotubes; conductivity, toughness and wear resistance were each improved by more than an order of magnitude. DSC measurements showed no evidence that the nanotube surfaces induced any response by the PTFE. Rather, the dramatic improvements were attributed to nanotube networking, mechanical immobilization of the PTFE and the novel properties of the nanotubes themselves.

(1) Electrical resistance dropped by several orders of magnitude at 2 wt.% SWCNT loading and decreased monotonically with increased filler loading under a 200 V potential. The presence of electrically conductive pathways indicates inter-nanotube contact (percolation) over macroscopic distances.
(2) The nanotubes led to a significant increase in toughness; 2 wt.% SWCNTs increased strength by ∼50% and strain by ∼8000%.
(3) At all loadings, the nanotubes increased wear resistance by more than 2000%. At low speed, the friction coefficients of the nanocomposite were approximately 50% higher than that of unfilled PTFE. However, the nanocomposites are less speed sensitive than unfilled PTFE and friction coefficients can be lower at speeds typical of engineering applications.
(4) The nanotubes had no effect on PTFE crystallinity. The dramatic property improvements were attributed to nanotube networking, mechanical immobilization of the PTFE and the novel properties of the nanotubes themselves.

Acknowledgements

This material is based upon an AFOSR-MURI grant FA9550-04-1-0367. Any opinions, findings, and conclusions or recommendations expressed in this material are those of the authors and do not necessarily reflect the views of the Air Force Office of Scientific Research.

References

[1] A. Eitan, F. Fisher, R. Andrews, L. Brinson, L. Schadler, Reinforcement mechanisms in MWCNT-filled polycarbonate, Composites Science and Technology 66 (2006) 1162–1173.
[2] P. He, Y. Gao, J. Lian, L. Wang, D. Qian, J. Zhao, W. Wang, M. Schulz, X. Zhou, D. Shi, Surface modification and ultrasonication effect on the mechanical properties of carbon nanofiber/polycarbonate composites, Composites Part A: Applied Science and Manufacturing 37 (2006) 1270–1275.
[3] A. Mierczynska, M. Mayne-L'Hermite, G. Boiteux, J.K. Jeszka, Electrical and mechanical properties of carbon nanotube/ultrahigh-molecular-weight polyethylene composites prepared by a filler prelocalization method, Journal of Applied Polymer Science 105 (2007) 158–168.
[4] E.T. Thostenson, C.Y. Li, T.W. Chou, Nanocomposites in context, Composites Science and Technology 65 (2005) 491–516.
[5] E.T. Thostenson, Z.F. Ren, T.W. Chou, Advances in the science and technology of carbon nanotubes and their composites: a review, Composites Science and Technology 61 (2001) 1899–1912.
[6] D. Wagner, R. Vaia, Nanocomposites: issues at the interface, Materials Today (2004) 38–42.

[7] S.M. Aouadi, Y. Paudel, B. Luster, S. Stadler, P. Kohli, C. Muratore, C. Hager, A.A. Voevodin, Adaptive $Mo_2N/MoS_2/Ag$ tribological nanocomposite coatings for aerospace applications, Tribology Letters 29 (2008) 95–103.
[8] D. Burris, W. Sawyer, Improved wear resistance in alumina–PTFE nanocomposites with irregular shaped nanoparticles, Wear 260 (2006) 915–918.
[9] D. Burris, W. Sawyer, A low friction and ultra low wear rate PEEK/PTFE composite, Wear 261 (2006) 410–418.
[10] D.L. Burris, B. Boesl, G.R. Bourne, W.G. Sawyer, Polymeric nanocomposites for tribological applications, Macromolecular Materials and Engineering 292 (2007) 387–402.
[11] J.J. Hu, C. Muratore, A.A. Voevodin, Silver diffusion and high-temperature lubrication mechanisms of YSZ–Ag–Mo based nanocomposite coatings, Composites Science and Technology 67 (2007) 336–347.
[12] N. McCook, D. Burris, G. Bourne, J. Steffens, J. Hanrahan, W. Sawyer, Wear resistant solid lubricant coating made from PTFE and epoxy, Tribology Letters 18 (2005) 119–124.
[13] C. Muratore, A.A. Voevodin, Molybdenum disulfide as a lubricant and catalyst in adaptive nanocomposite coatings, Surface & Coatings Technology 201 (2006) 4125–4130.
[14] C. Muratore, A.A. Voevodin, J.J. Hu, J.S. Zabinski, Tribology of adaptive nanocomposite yttria-stabilized zirconia coatings containing silver and molybdenum from 25 to 700 degrees C, Wear 261 (2006) 797–805.
[15] C. Muratore, A.A. Voevodin, J.J. Hu, J.S. Zabinski, Multilayered YSZ–Ag–Mo/TiN adaptive tribological nanocomposite coatings, Tribology Letters 24 (2006) 201–206.
[16] N. McCook, D. Burris, P. Dickrell, W. Sawyer, Cryogenic friction behavior of PTFE based solid lubricant composites, Tribology Letters 20 (2005) 109–113.
[17] C. Muratore, A.A. Voevodin, J.J. Hu, J.G. Jones, J.S. Zabinski, Growth and characterization of nanocomposite yttria-stabilized zirconia with Ag and Mo, Surface & Coatings Technology 200 (2005) 1549–1554.
[18] C. Muratore, J.J. Hu, A.A. Voevodin, Adaptive nanocomposite coatings with a titanium nitride diffusion barrier mask for high-temperature tribological applications, Thin Solid Films 515 (2007) 3638–3643.
[19] S. McElwain, Wear Resistant PTFE Composites via Nano-Scale Particles, Master's Thesis, Rensselaer Polytechnic Institute, Troy, New York, 2006.
[20] S. McElwain, T. Blanchet, L. Schadler, W. Sawyer, Effect of particle size on the wear resistance of alumina-filled PTFE micro- and nanocomposites, Tribology Transactions 51 (2008) 247–253.
[21] W. Chen, F. Li, G. Han, J. Xia, L. Wang, J. Tu, Z. Xu, Tribological behavior of carbon–nanotube-filled PTFE composites, Tribology Letters 15 (2003) 275–278.
[22] W. Sawyer, K. Freudenberg, P. Bhimaraj, L. Schadler, A study on the friction and wear behavior of PTFE filled with alumina nanoparticles, Wear 254 (2003) 573–580.
[23] T. Schmitz, J. Action, D. Burris, J. Ziegert, W. Sawyer, Wear-rate uncertainty analysis, Journal of Tribology-Transactions of the ASME 126 (2004) 802–808.
[24] T. Schmitz, J. Action, J. Ziegert, W. Sawyer, The difficulty of measuring low friction: uncertainty analysis for friction coefficient measurements, Journal of Tribology-Transactions of the ASME 127 (2005) 673–678.
[25] T. Agag, T. Koga, T. Takeichi, Studies on thermal and mechanical properties of polyimide-clay nanocomposites, Polymer 42 (2001) 3399–3408.
[26] B. Ash, L. Schadler, R. Siegel, Glass transition behavior of alumina/polymethylmethacrylate nanocomposites, Materials Letters 55 (2002) 83–87.
[27] D. Ratna, S. Divekar, A. Samui, B. Chakraborty, A. Banthia, Poly(ethylene oxide)/clay nanocomposite: thermomechanical properties and morphology, Polymer 47 (2006) 4068–4074.
[28] A. Yasmin, J. Luo, J. Abot, I. Daniel, Mechanical and thermal behavior of clay/epoxy nanocomposites, Composites Science and Technology 66 (2006) 2415–2422.
[29] A. Zhu, S. Sternstein, Nonlinear viscoelasticity of nanofilled polymers: interfaces, chain statistics and properties recovery kinetics, Composites Science and Technology 63 (2003) 1113–1126.
[30] D.L. Burris, Effects of Nanoparticles on the Wear Resistance of Polytetrafluoroethylene, Doctoral Thesis, University of Florida, Gainesville Florida, 2007.
[31] M.F. Mu, A.M. Walker, J.M. Torkelson, K.I. Winey, Cellular structures of carbon nanotubes in a polymer matrix improve properties relative to composites with dispersed nanotubes, Polymer 49 (2008) 1332–1337.
[32] M.K. Seo, S.J. Park, Electrical resistivity and rheological behaviors of carbon nanotubes-filled polypropylene composites, Chemical Physics Letters 395 (2004) 44–48.
[33] A. Ltaief, A. Bouazizi, J. Davenas, R. Ben Chaabane, H. Ben Ouada, Electrical and optical properties of thin films based on Meh-Ppv/fullerene blends, Synthetic Metals 147 (2004) 261–266.
[34] T. Blanchet, F. Kennedy, Sliding wear mechanism of polytetrafluoroethylene (PTFE) and PTFE composites, Wear 153 (1992) 229–243.
[35] K. Makinson, D. Tabor, Friction + transfer of polytetrafluoroethylene, Nature 201 (1964) 464.
[36] K. McLaren, D. Tabor, Visco-elastic properties and friction of solids – friction of polymers – influence of speed and temperature, Nature 197 (1963) 856.
[37] K. Tanaka, Y. Uchiyama, S. Toyooka, Mechanism of wear of polytetrafluoroethylene, Wear 23 (1973) 153–172.
[38] S.F. Lau, H. Suzuki, B. Wunderlich, The thermodynamic properties of polytetrafluoroethylene, Journal of Polymer Science Part B: Polymer Physics 22 (1984) 379–405.
[39] H. Ting-Yung, N. Eiss, Effects of molecular weight and crystallinity on wear of polytetrafluoroethylene, Wear of Materials: International Conference on Wear of Materials 2 (1983) 636–642.
[40] J. Lancaster, Polymer-based bearing materials—role of fillers and fiber reinforcement in wear, Wear 22 (1972) 412.
[41] N. Sung, N. Suh, Effect of fiber orientation on friction and wear of fiber reinforced polymeric composites, Wear 53 (1979) 129–141.
[42] T. Blanchet, A model for polymer composite wear behavior including preferential load support and surface accumulation of filler particulates, Tribology Transactions 38 (1995) 821–828.
[43] O. Lin, Z. Ishak, H. Akil, Preparation and properties of nanosilica-filled polypropylene composites with PP-Methyl POSS as compatibiliser, Materials and Design 30 (2009) 748–751.
[44] H. Lu, Y. Hu, M. Li, Z. Chen, W. Fan, Structure characteristics and thermal properties of silane-grafted-polyethylene/clay nanocomposite prepared by reactive extrusion, Composites Science and Technology 66 (2006) 3035–3039.